Journal of Organometallic Chemistry 880 (2019) 75–82

Contents lists available at ScienceDirect

Journal of Organometallic Chemistry

journal homepage: www.elsevier.com/locate/jorganchem

Ultrasound-promoted an efficient method for the one-pot synthesis of indeno fused pyrido[2,3-d]pyrimidines catalyzed by $H_3PW_{12}O_{40}$ functionalized chitosan@Co_3O_4 as a novel and green catalyst

Javad Safari [a, *], Mona Tavakoli [a], Mohammad Ali Ghasemzadeh [b]

[a] Department of Organic Chemistry, Faculty of Chemistry, University of Kashan, Kashan, 87317, Iran
[b] Department of Chemistry, Qom Branch, Islamic Azad University, Qom, Iran

ARTICLE INFO

Article history:
Received 5 September 2018
Received in revised form
24 October 2018
Accepted 28 October 2018
Available online 1 November 2018

Keywords:
Heterogeneous catalyst
Co_3O_4/CS/PWA
Three-component reaction
Ultrasound irradiation
Indeno[2′;,1′;:5,6]pyrido[2,3-d]pyrimidine

ABSTRACT

A novel magnetically recoverable nanocomposite including Co_3O_4/chitosan/$H_3PW_{12}O_{40}$ (Co_3O_4/CS/PWA) as a heterogeneous catalyst was prepared using a facile synthetic method and characterized by FT-IR, XRD, SEM, VSM and EDX. A simple, efficient and rapid synthesis of indeno[2′,1′:5,6]pyrido[2,3-d]pyrimidines was accomplished in excellent yields via one-pot three-component reaction of 1,3-dimethyl-6-aminouracil, aryl aldehydes and 1,3-indandione in the presence of amount of Co_3O_4/CS/PWA catalyst under ultrasound irradiation. Then, the catalyst was recovered with an external magnet and reused several times without significant loss of reactivity.

1. Introduction

Nano catalysts have attracted considerable attention in catalysis science. This attention can be attributed to their efficient recovery characteristics, recycling potential, highly stability, selectivity, activity and durability in the catalytic activities [1]. These characteristics are affected by size, shape, morphology, composition, electronic structure and composition and can also affect the catalytic activity of a material [2].

Recently, magnetic nanoparticles (MNPs) has been applied as an effective heterogeneous catalyst with a number of advantages such as control of nanoparticle size, shape and activity, enhanced selectivity, active sites, ease of availability, excellent thermal stability and chemical inertness [3–7]. In addition, these magnetic nanoparticles reduces energy consumption and saves time in achieving catalyst recovery through facile separation from the reaction mixture by an external magnet [8,9]. Cobalt oxide nanoparticles (Co_3O_4 NPs) are currently attracting enormous interest owing to their unique size and shape-dependent properties and potential applications in battery cathodes, magnetic materials, electrochromic devices, solid-state sensors and catalysis [10–14].

Chitosan is a random copolymer of glucosamine and an N-acetyl glucosamine linked, obtained after partial deacetylation of chitin, which is a byproduct of seafood processing industries [15,16]. It is a natural, commercially available, eco-friendly, chemically stable, biocompatibility, non-toxicity, antioxidant properties, low immunogenicity and inhibits the growth of a wide variety of bacteria and fungi [17–19]. The amino and hydroxyl groups in the repeating glycosidic residue provides various coordination sites for chemical modifications and a suitable matrix to synthesize magnetic composites [20].

The materials such as Fe_3O_4 [15,16,18], Cu [21–23], Ag [24], Ni nanoparticles [25] and magnetic carbon nanotube [26] are as a core in the network of the cross-linked chitosan, extensively prepared and used in catalytic reaction therefore employed for carbonylation, oxidation, C–C coupling and multicomponent reactions [16,27].

Heteropolyacids (HPAs) are important class of compounds that are widely used as catalyst for the synthesis of fine and specific chemicals, medicine, and materials science [28]. These compounds possess unique properties such as high thermal stability, high proton mobility, high oxidation potential, easy work-up procedures, safety, easy separability, little waste and easy filtration

* Corresponding author.
E-mail addresses: safari_jav@yahoo.com, safari@kashanu.ac.ir (J. Safari).

https://doi.org/10.1016/j.jorganchem.2018.10.028
0022-328X/

[29–32]. HPAs are well known super-strong acids for both homogeneous and heterogeneous acid-catalyzed reactions [33]. $H_3PW_{12}O_{40}$ (12-phosphotungstic acid; PWA), the free acidic forms of HPWs with Keggin structure, is considered for chemical conversions because of their strong Brønsted acidity and higher stability [34].

Ultrasonic-assisted organic synthesis (UAOS) as a green synthetic approach is a promising technique that is being used in the chemistry process which requires drastic conditions or prolonged reaction time [10,35]. UAOS can be extremely efficient and it is applicable to an approach are enhanced reaction rates, formation of purer products in high yields, easier manipulation and environmental friendliness which compared with traditional methods [16,36].

Pyrido[2,3-*d*]pyrimidines are an important class of heterocyclic compounds annulated uracil with wide range of biological and pharmacological activities, such as anti-folate, anticonvulsants, anti-bacterial, antimicrobial, anti-inflammatory, anti-aggressive activity, anti-leishmania and inhibitors of cyclin-dependent kinases [37,38].

The synthesis of indeno[2′,1′:5,6]Pyrido[2,3-*d*]pyrimidines have already been reported via multicomponent reactions in the presence of *β*-cyclodextrin-propyl sulfonic acid [39], *p*-toluene sulfonic acid [40], indium trichloride [41], zirconium hydrogen sulfate [42] and Fe_3O_4@SiO_2–SO_3H [43] as catalyst.

In this work, we designed the construction of a magnetically recoverable acid nanocomposite, in which $H_3PW_{12}O_{40}$ (12-phosphotungstic acid) molecules are immobilized into the network of the cross-linked chitosan with the paramagnetic Co_3O_4 nanoparticles as a novel, green and recyclable catalyst (Scheme 1).

2. Experimental

All chemicals used in this work from Merck or Aldrich Chemical Company.

FT-IR spectra were obtained with KBr pellets in the range 400–4000 cm^{-1} with a Perkin-Elmer 550 spectrometer. ^1H NMR spectra was obtained using a Bruker DRX-400 AVANCE spectrometer at 400 MHz. Melting points were determined using an Electrothermal 9100 apparatus and are uncorrected. Nanostructures were characterized using a Holland Philips X ray powder diffraction (XRD) diffractometer (Cu K, radiation, k = 0.154056 nm), at a scanning speed of 2 min1 from 10 to 100 (2Θ). Microscopic Morphological characteristics were observed By SEM (LEO 1455VP). Magnetic properties were characterized by a vibrating sample magnetometer (VSM, MDKFD, University of kashan, Kashan, Iran) at room temperature. The compositional analysis was done by energy-dispersive analysis of X-ray (EDX, Kevex, Delta Class I). Sonication was performed in a Shanghai Branson-BUG40-06 ultrasonic cleaner (with a frequency of 40 kHz and anominal power of 200 W).

2.1. Preparation of Co_3O_4 nanoparticles

Co_3O_4 MNPs were prepared according to previously reported procedure by Vela et al. with some modifications [44]. First, cobalt nitrate hexahydrate (8.60 g) was dissolved in 100 ml of ethanol the mixture was vigorously stirred. Then, the mixture was heated to 50 °C and kept for 30 min. Finally, oxalic acid (2.14 g) was added quickly to the solution and the reaction mixture was stirred for 2 h at 50 °C. The formed precipitate including cobalt (II) oxalate was collected by centrifuge, followed by calcination at 400 °C for 2 h to produce the Co_3O_4 nanoparticles.

2.2. Preparation of $H_3PW_{12}O_{40}$

$H_3PW_{12}O_{40}$ was synthesized by the addition of Na_2WO_4 (50 g) in 75 ml H_2O to a solution of 1 ml of H_3P0_4 (85%). The solution was stirred and heated to boiling point followed by addition of HCl. The hot mixed liquid was filtrated through Buchner funnel and transferred to a separator funnel after it has been cooled at room temperature and added 30 ml ether. And finally, it was placed in thermostatic oven with a temperature of 110 °C and dried until the solvent had been evaporated, obtained $H_3PW_{12}O_{40}$ [45]. Principle can be expressed as reaction equation (1):

$$PO_4^{3-} + 12WO_4^{2-} + 24\ H^+ \rightarrow H_3PW_{12}O_{40} + 12H_2O \quad (1)$$

2.3. Procedure for the preparation of Co_3O_4/chitosan/HPA

For the synthesis of chitosan–Co_3O_4 core-shell (CS–Co_3O_4), 0.5 g of Co_3O_4 nanoparticles was added to a solution containing 0.5 g of chitosan in 50 mL of acetic acid (0.05 M) solution. The mixture was sonicated and heated at 40 °C for 0.5 h, After that, 12 ml of 4 wt% glutaraldehyde aqueous solutions was added drop by drop under stirring and the reactant mixtures were heated and stirred for 1 h at 40 °C and 1 h at 60 °C. The cross-linking chitosan-coated Co_3O_4 (CS–Co_3O_4) was formed in the process. Then, 20 ml of aqueous solution containing $H_3PW_{12}O_{40}$ (12-phosphotungstic acid) (0.045 g mL^{-1}) was added to the mixture and stirred for 0.5 h at

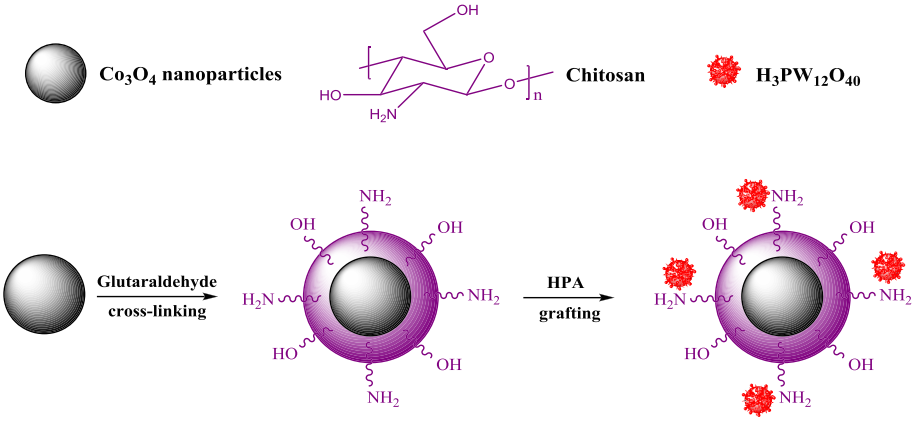

Scheme 1. Preparation process of Co_3O_4/chitosan/HPA.

60 °C. Finally, the black gel products were separated by centrifugation, washed several times with deionized water and ethanol and dried in vacuum at 60 °C for 8 h.

2.4. General procedure for the synthesis of indeno fused pyrido[2,3-d]pyrimidines

A mixture of 1,3-dimethyl-6-aminouracil (1 mmol), aryl aldehyde (1 mmol), 1,3-indandione (1 mmol) in EtOH (5 ml) was irradiated in the ultrasonic bath in the presence of Co_3O_4/CS/HPA (0.005 g). After the completion of the reaction (monitored by TLC), the reaction was allowed to cool and the magnetic catalyst was removed by an external magnet. The obtained solid was filtered, cooled and washed with water and ethanol to afford the desired pure product.

2.5. Spectral data for new compounds

2.5.1. 4-(1,3-Dimethyl-2,4,6-trioxo-2,3,4,5,6,11-hexahydro-1H-indeno[2′,1′:5,6]pyrido[2,3-d]pyrimidin-5-yl)benzonitrile (4i)

m.p = > 300 °C; Yellow solid; IR (KBr, cm^{-1}): 3424, 2958, 1715, 1661, 1573, 1504; ^{1}H NMR (400 MHz, DMSO-d_6) δ: 3.14 (s, 3H, CH_3), 3.75 (s, 3H, CH_3), 7.45 (d, J = 6.8 Hz, 2H, Ar-H), 7.60–7.66 (m, 2H, Ar-H), 7.78 (t, J = 6.1 Hz, 1H, Ar-H), 7.88 (d, J = 6.4 Hz, 2H, Ar-H), 7.99 (d, J = 6.0 Hz, 1H, Ar-H) ppm; Anal. Calcd (%) for $C_{23}H_{14}N_4O_3$: C, 70.05; H, 3.58; N, 14.21. Found: C, 69.9; H, 3.69; N, 14.13.

2.5.2. 5-(3-bromophenyl)-1,3-dimethyl-1H-indeno[2′,1′:5,6]pyrido[2,3-d]pyrimidine-2,4,6(3H)-trione (4j)

m.p = > 300 °C; Yellow solid; IR (KBr, cm^{-1}): 3417, 3067, 1718, 1673, 1567, 1500; ^{1}H NMR (400 MHz, DMSO-d_6) δ: 3.14 (s, 3H, CH_3), 3.73 (s, 3H, CH_3), 7.23 (d, J = 7.6 Hz, 1H, Ar-H), 7.36 (t, J = 7.6 Hz, 1H, Ar-H), 7.44 (s, 1H, Ar-H), 7.61 (t, J = 7.2 Hz, 3H, Ar-H), 7.77 (t, J = 7.2 Hz, 1H, Ar-H), 7.97 (d, J = 7.2 Hz, 1H, Ar-H) ppm; Anal. Calcd (%) for $C_{22}H_{14}BrN_3O_3$: C, 58.95; H, 3.15; N, 9.37. Found: C, 58.90; H, 3.18; N, 9.33.

2.5.3. 5-(2-chlorophenyl)-1,3-dimethyl-1H-indeno[2′,1′:5,6]pyrido[2,3-d]pyrimidine-2,4,6(3H)-trione (4k)

m.p = > 300 °C; Orange solid; IR (KBr, cm^{-1}): 3433, 2922, 1700, 1659, 1629, 1504; ^{1}H NMR (400 MHz, DMSO-d_6) δ: 3.06 (s, 3H, CH_3), 3.59 (s, 3H, CH_3), 5.18 (s, 1H, CH), 7.12 (d, J = 7.6 Hz, 1H, Ar-H), 7.18 (t, J = 7.2 Hz, 1H, Ar-H), 7.22 (d, J = 7.2 Hz, 1H, Ar-H), 7.26 (d, J = 8.0 Hz, 1H, Ar-H), 7.33 (t, J = 7.2 Hz, 2H, Ar-H), 7.47 (t, J = 7.2 Hz, 1H, Ar-H), 7.87 (d, J = 6.8 Hz, 1H, Ar-H) ppm; Anal. Calcd (%) for $C_{22}H_{14}ClN_3O_3$: C, 65.44; H, 3.49; N, 10.41. Found: C, 65.41; H, 3.52; N, 10.39.

3. Results and discussion

The magnetically heterogeneous nanocomposite Co_3O_4/CS/HPA, is characterized by Fourier transform infrared (FT-IR), X-ray diffraction (XRD), scanning electron microscopy (SEM), vibrating sample magnetometer (VSM) and energy-dispersive X-ray spectroscopy (EDX). The FTIR spectra of Co_3O_4 nanoparticles, chitosan, $H_3PW_{12}O_4$, magnetic Co_3O_4/CS/HPA catalyst are shown in Fig. 1. The two strong absorption bands at 567 and 664 cm^{-1} are attributed to the vibrations of Co–O in Co_3O_4 nanoparticles (Fig. 1a). In Fig. 1b the main bands of chitosan were characterized by the following absorption bands: coaxial stretching vibration of O–H overlapped with N–H stretching visible at 3000–3750 cm^{-1}, C–O of hydroxyl group at 1383 cm^{-1}. Also, the C–H axial stretching band appears at 2922 cm^{-1} [15–18]. The characteristic bands of $H_3PW_{12}O_{40}$ are clearly observed at P–O stretching at 1079 cm^{-1}, a band at 983 cm^{-1} corresponding to W=O and band at 891 and 792 cm^{-1} due to W–O_c–W and W–O_b–W respectively (Fig. 1c) [46,47]. In the FTIR spectrum of Co_3O_4/CS/HPA, the absorption peaks of Co–O bonds at 569 and 663 cm^{-1} indicates the successful cross-linking of chitosan on the Co_3O_4 particle surface. The stretching vibration characteristic peak of C=N at 1628 cm^{-1} is due to cross-linking reaction by glutaraldehyde. The broad band at 3150–3700 cm^{-1} is due to the hydroxyl (O–H) stretching in Co_3O_4/CS/HPA. In addition, the characteristic IR bands of $H_3PW_{12}O_{40}$ were clearly observed in the IR spectrum of the as-prepared Co_3O_4/CS/HPA catalyst at 1079, 954, 889 and 807 cm^{-1}. The results are consistent with the synthesis design, and confirm that $H_3PW_{12}O_{40}$ are highly dispersed on the net cross-linking chitosan in the singular molecule form (Fig. 1d).

The X-ray diffraction patterns of Co_3O_4 nanoparticles and Co_3O_4/CS/HPA are shown in Fig. 2. The particle size of Co_3O_4 nanoparticles is determined to be about 25 nm by Scherrer's equation (K = 0.90). As can be seen, the XRD pattern Co_3O_4/CS/HPA catalyst reveals the same diffraction peaks to that of bare Co_3O_4.

The morphology, size and shape of the catalyst were studied by scanning SEM (Fig. 3). It showed that magnetic Co_3O_4/CS/HPA nanocomposite are nearly spherical with diameter about 20–40 nm, which is completely agreement with the XRD spectrum.

The magnetic properties of the uncoated Co_3O_4 and Co_3O_4/CS/HPA nanocomposite were measured with VSM (Fig. 4). There are no

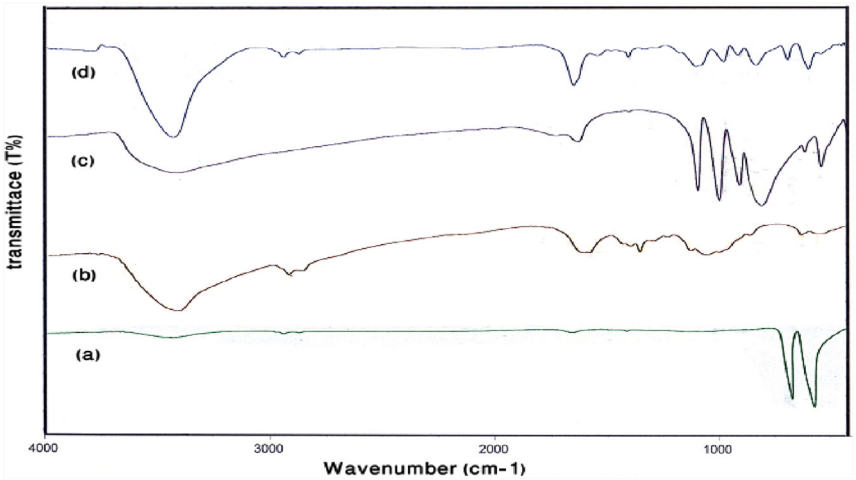

Fig. 1. FT-IR spectra of Co_3O_4 NPs (a), chitosan (b), $H_3PW_{12}O_{40}$ (c), Co_3O_4/CS/HPA (d).

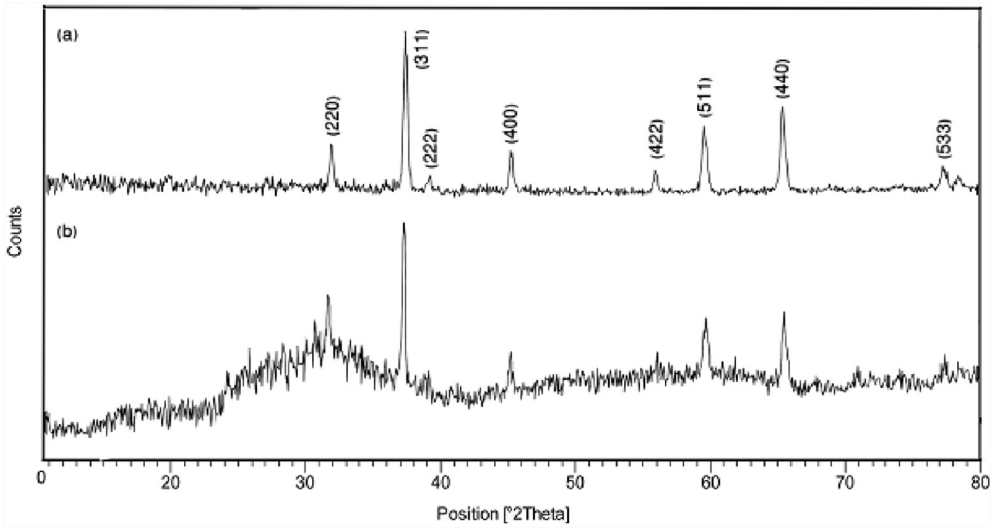

Fig. 2. X-ray diffraction of Co_3O_4 NPs (a) and Co_3O_4/CS/HPA catalyst (b).

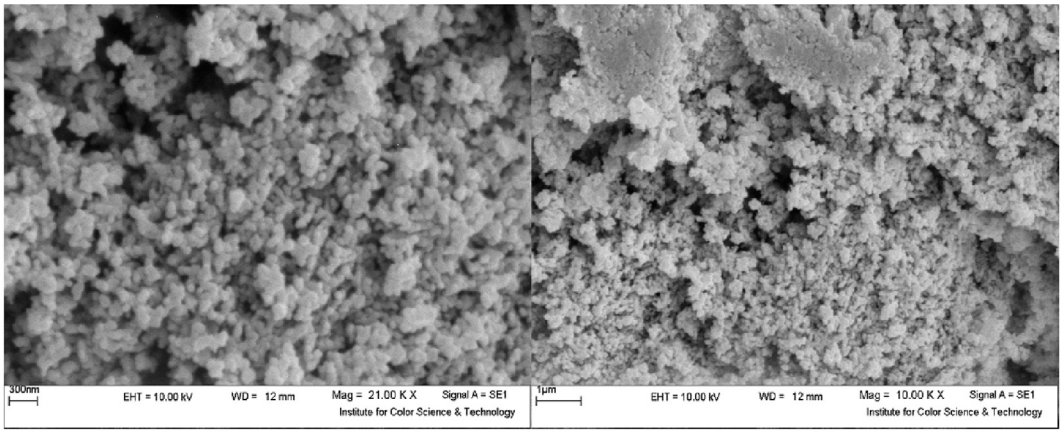

Fig. 3. SEM images of Co_3O_4/CS/HPA catalyst.

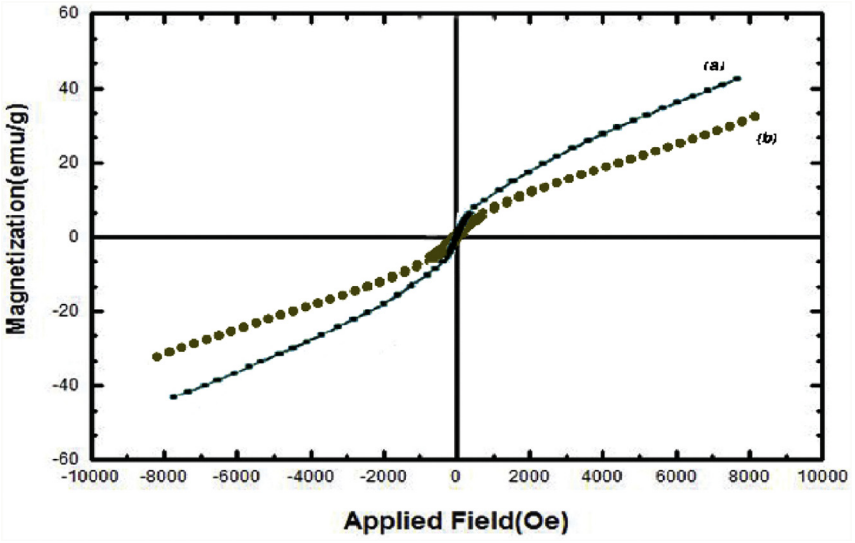

Fig. 4. VSM magnetization curves of the Co_3O_4 NPs (a) and Co_3O_4/CS/HPA (b).

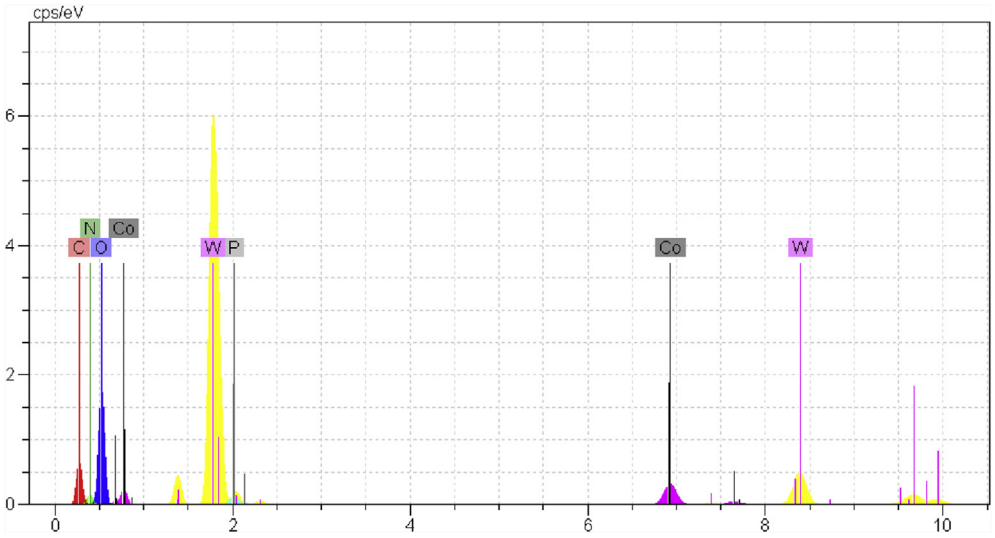

Fig. 5. EDX spectra of Co_3O_4/CS/HPA catalyst.

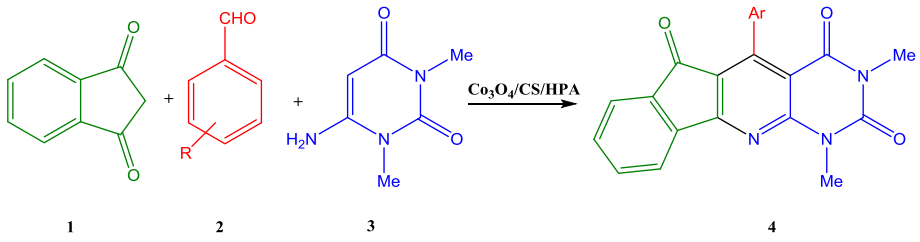

Scheme 2. Three-component synthesis of indeno[2′,1′:5,6]pyrido[2,3-d]pyrimidine by Co_3O_4/CS/HPA nanocomposite.

hysteresis, coercivity and remanence in bare Co_3O_4 and Co_3O_4/CS/HPA samples at room temperature that show their typical superparamagnetic properties. The decrease in magnetic saturation for Co_3O_4/CS/HPA is attributed to the cover of CS/HPA hybrid materials shells on the surface of magnetic Co_3O_4 MNPs cores.

The chemical purity of the catalyst was tested by energy-dispersive X-ray spectroscopy (EDX). As shown in Fig. 5, the EDX spectrum shows the presence of Co, W, C, O, N and P as the elements of the nanocomposites.

In this research, we report an efficient synthesis of indeno[2′,1′:5,6]pyrido[2,3-d] pyrimidines in high yields via the cyclo-condensation reactions in the presence of Co_3O_4/CS/HPA as an efficient catalyst under ultrasound irradiation. In order to optimize the reaction conditions, the model reaction was carried out using 1,3 -indandione **1**, aldehyde (R = 4-Cl), **2** and 1,3-dimethyl-6-aminouracil **3** under various conditions by using ultrasound irradiation (Scheme 2). The reaction conditions were optimized on the basis of the solvent, catalyst, and different intensity power of ultrasonic for the synthesis of indeno[2′,1′:5,6]pyrido[2,3-d] pyrimidine.

To determine the effect of different solvents on the model reaction, the reaction was carried out in a range of different solvents such as: MeOH, EtOH, CH_2Cl_2, CCl_4, and CH_3CN. It was found that CCl_4 was completely ineffective for the reaction, with no trace amount of the product being detected. CH_2Cl_2 and CH_3CN were also

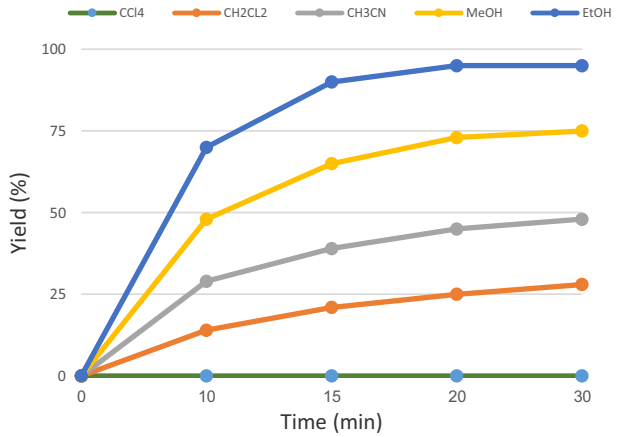

Fig. 6. Effect of different solvents on model reaction.

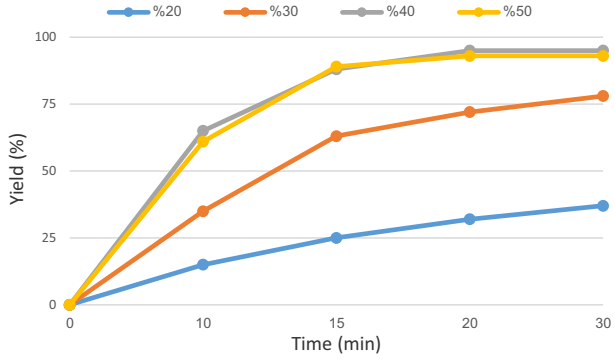

Fig. 7. Effect of intensity power of ultrasonic on the synthesis of indeno[2′,1′:5,6]pyrido[2,3-d] pyrimidine.

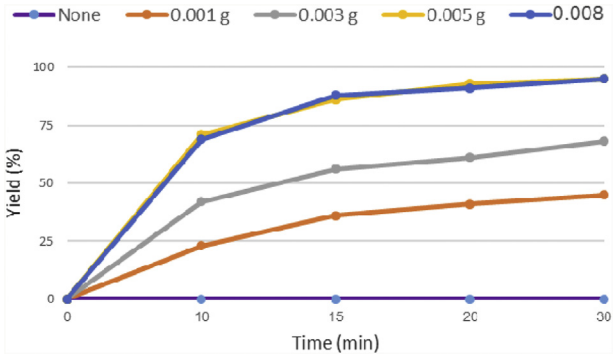

Fig. 8. Effect of amount catalyst on reaction yield.

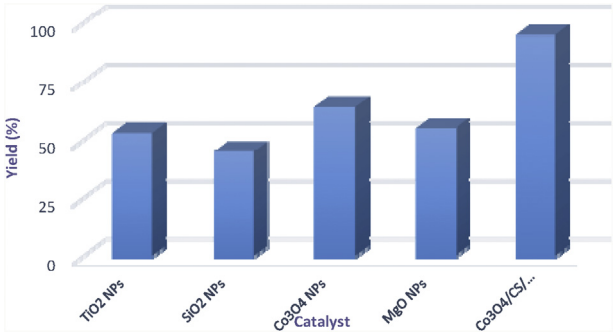

Fig. 9. Effect of various catalysts on the model study.

unsuitable for the reaction, affording only 28% and 48% conversion after 30 min, respectively. MeOH offered better performance than CH_2Cl_2 and CH_3CN, with 75% conversions, being observed after 30 min. Among these solvents, EtOH exhibited the best performance, and should be the solvent of choice for the reaction conversion to 95% after 30 min using the Co_3O_4/CS/HPA catalyst under ultrasound irradiation (Fig. 6).

After this, we have studied the effect of intensity power of ultrasonic on the model reaction. The model study was carried out at 20%, 30%, 40% and 50% of the rate power of the ultrasonic bath (40, 60, 80 and 100 W).

The results are shown in Fig. 7. Generally, the enhance in the acoustic power could enhance the number of active cavitation bubbles and also the size of the individual bubbles. Both increases can be supposed to result in an increase in the maximum collapse temperature and the respective reaction could be done faster. It can be seen from Fig. 7 that increase of ultrasonic power led to relatively higher yield and shorter reaction time before the ultrasound power intensity reached 40%, and then the yield decreased slightly with increasing ultrasound power intensity.

In continuation of our research, the model reaction was carried out in the range of 0–0.008 g of Co_3O_4/CS/HPA nanocomposite. According to Fig. 8, no product was obtained in the absence of the catalyst, confirming the necessity of using the Co_3O_4/CS/HPA for the reaction conditions. It was found that the optimum amount of catalyst was 0.005 g catalyst which proceeded readily to 95% conversion after 30 min. Also the results indicate that decreasing in the amounts of the catalyst from 0.005 g led to decrease in yield of the reaction. It should be noted that increasing of the catalyst did not show any significant changes in yield and time of reaction.

In order to study the effect of various catalysts under ultrasound irradiation, catalytic behaviors of five types of catalysts such as TiO_2 NPs, SiO_2 NPs, Co_3O_4 NPs, MgO NPs and Co_3O_4/CS/HPA were investigated on the model reaction (Fig. 9). When TiO_2 NPs, SiO_2 NPs, Co_3O_4 NPs and MgO NPs was used as the catalyst, the reaction could proceed to 53%, 45%, 64%, 55% conversion after 30 min, respectively. The result of this study showed that compound provided high yield in the presence of the Co_3O_4/CS/HPA nanocomposites under ultrasound irradiation.

A plausible mechanism for the reaction by catalysis of Co_3O_4/CS/HPA nanocomposite is shown in Scheme 3. We suppose that Co_3O_4/CS/HPA behave as strong acid by increasing the electrophilicity of

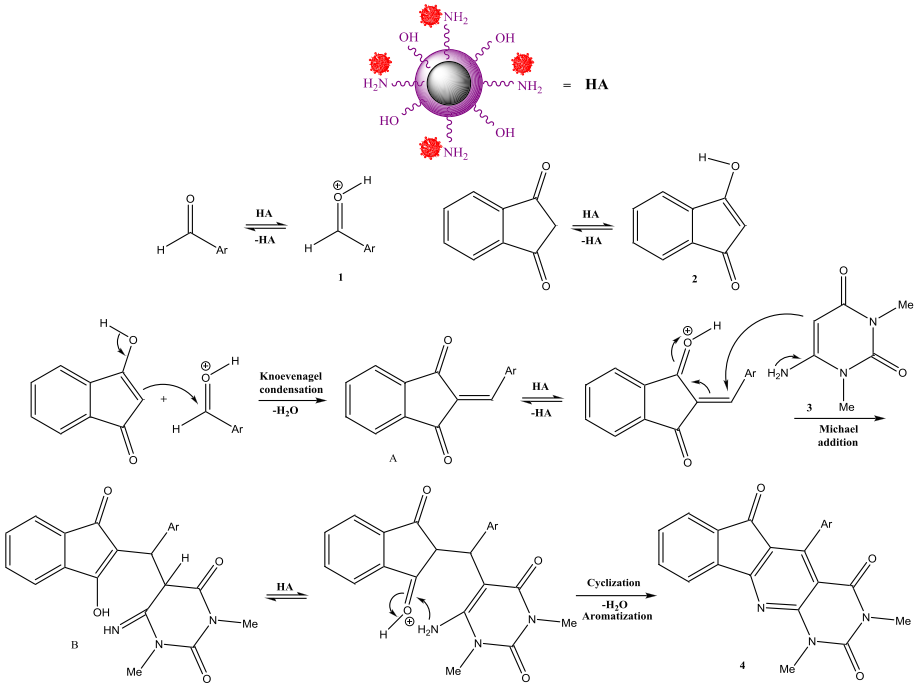

Scheme 3. Plausible mechanism of the reaction.

Table 1
Synthesis of indeno[2′,1′:5,6]pyrido[2,3-d]pyrimidine derivatives by using Co_3O_4/CS/HPA nanocomposite as catalyst under ultrasound irradiation.[a].

Yield of 4 (%)[b]	Time (min)	Product	R	Entry
86	30	4a	H	1
90	25	4b	4-Br	2
80	30	4c	*4-i*-Propyl	3
83	25	4d	2-NO2	4
88	30	4e	4-CH3	5
92	30	4f	4-NO2	6
85	25	4g	3-NO2	7
95	30	4h	4-Cl	8
90	20	4i	4-CN	9
86	25	4j	3-Br	10
81	30	4k	2-Cl	11

[a] Reaction conditions: various aldehydes (1 mmol), 1,3-indandione (1 mmol) and 1,3-dimethyl-6- aminouracil (1 mmol), catalyst (0.005 g) at 40 °C under ultrasound irradiation.
[b] Yields of isolated products.

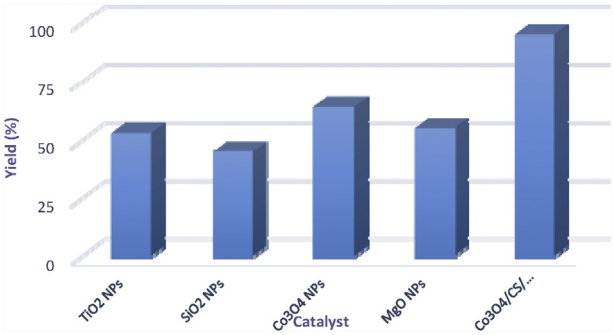

Fig. 10. Reusability of the Co_3O_4/CS/HPA nanocomposite.

carbonyl groups and intermediates, through formation of a strong coordinate band. As shown in Scheme 3, first, the activated carbonyl (**1**) reacts with activated 1,3-indandione (**2**) to afford the intermediate A which followed by a Michael-type addition reaction with 1,3-dimethyl-6-aminouracil (**3**) to produce the intermediate B. Subsequently, intramolecular cyclization, dehydration and aromatization on intermediate provided the final product.

To study the scope of this procedure, we have synthesized indeno[2′,1′:5,6]pyrido[2,3 d]pyrimidine derivatives by using a wide range of aromatic aldehydes containing electron-withdrawing and electron-donating groups in the presence of 0.005 g of Co_3O_4/CS/HPA nanocomposite. The results in Table 1 indicate that the aryl aldehydes with electron-donating groups required prolonged reaction time to give the yields, while the aryl aldehydes with electron-withdrawing groups reacted very smoothly and produced high yields of products.

In order to investigate the reusability of the catalyst, the model reaction was repeated using recovered Co_3O_4/CS/HPA core–shell nanocomposite under the optimized reaction conditions. After completing the model reactions, the products were removed by filtration. The catalyst was separated magnetically and then washed with water and ethanol. As shown in Fig. 10, we observed that the separated catalyst could be used for six cycles with a slightly decreased activity.

4. Conclusions

In summary, an efficient method for the synthesis of the indeno [2′,1′:5,6]pyrido[2,3-d]pyrimidines is reported by the treatment of aryl aldehydes, 1,3-indandione with 1,3-dimethyl-6-aminouracil in the presence of Co_3O_4/CS/HPA nanocomposite under ultrasonic irradiation. This method provides several advantages such as clean reaction conditions, simple work-up procedure, shorter reaction time, excellent yields, and reusability of the catalyst. We expect this method will find extensive applications in the field of combinatorial chemistry, diversity-oriented synthesis and sonochemistry and drug discovery.

Acknowledgments

We gratefully acknowledge the financial support from the Research Council of the University of Kashan for supporting this work.

References

[1] R.M. Mohamed, D.L. McKinney, W.M. Sigmund, Mater. Sci. Eng. R. 73 (2012) 1–13. http://doi.org/10.1016/j.mser.2011.09.001.
[2] K. Hemalatha, G. Madhumitha, A. Kajbafvala, N. Anupama, R. Sompalle, S.M. Roopan, J. Nanomater. 2013 (2013) 1–23. http://doi.org/10.1155/2013/341015.
[3] R.J. White, R. Luque, V.L. Budarin, J.H. Clark, D.J. Macquarrie, Chem. Soc. Rev. 38 (2009) 481–494. https://doi.org/10.1039/b802654h.
[4] R. Hudson, Y. Feng, R.S. Varma, A. Moores, Green Chem. 16 (2014), 4493–4450, https://doi.org/10.1039/c3gc42640h.
[5] M.B. Gawande, A.K. Rathi, I.D. Nogueira, R.S. Varma, P.S. Branco, Green Chem. 15 (2013) 1895–1899. http://doi.org/10.1039/c3gc40457a.
[6] M.B. Gawande, P.S. Branco, R.S. Varma, Chem. Soc. Rev. 42 (2013) 3371–3393. http://doi.org/10.1039/c3cs35480f.
[7] V. Polshettiwar, R. Luque, A. Fihri, H. Zhu, M. Bouhrara, J.M. Basset, Chem. Rev. 111 (2011) 3036–3075. http://doi.org/10.1021/cr100230z.
[8] J.C. Colmenares, W. Ouyang, M. Ojeda, E. Kuna, O. Chernyayeva, D. Lisovytskiy, S. De, R. Luque, A.M. Balu, Appl. Catal., B 183 (2015) 107–112. http://doi.org/10.1016/j.apcatb.2015.10.034.
[9] M.J. Jacinto, P.K. Kiyohara, S.H. Masunaga, R.F. Jardim, L.M. Rossi, Appl. Catal. Gen. 338 (2008) 52–57. http://doi.org/10.1016/j.apcata.
[10] M.A. Ghasemzadeh, M.H. Abdollahi-Basir, Green Chem. Lett. Rev. 9 (2016) 156. http://doi.org/10.1080/17518253.2016.1204013.
[11] H. Qiao, L. Xiao, Z. Zheng, H. Liu, F. Jia, L. Zhang, J. Power Sources 185 (2008) 486–491. http://doi.org/10.1016/j.jpowsour.2008.06.096.
[12] L. Zhang, D. Xue, J. Mater. Sci. Lett. 21 (2002) 1931–1933. http://doi.org/10.1023/A:1021656529934.
[13] X. Xie, W. Shen, Nanoscale 1 (2009) 50–60. http://doi.org/10.1039/b9nr00155g.
[14] W.Y. Li, L.N. Xu, J. Chen, Adv. Funct. Mater. (2005) 851–857. http://doi.org/15.
[15] J. Safari, L. Javadian, RSC Adv. 4 (2014) 48973–48979. http://doi.org/10.1039/c4ra06618a.
[16] J. Safari, L. Javadian, Ultrason. Sonochem. 22 (2015) 341–348. http://doi.org/10.1039/c5ra23457c.
[17] J. Safari, F. Azizi, M. Sadeghi, New J. Chem. 39 (2015) 1905–1909. http://doi.org/10.1039/c4nj01730g.
[18] J. Safari, Z. Zarnegar, RSC Adv. 4 (2014) 20932–20939. http://doi.org/10.1039/c4ra03176h.
[19] Y. Xie, X. Liu, Q. Chen, Carbohydr. Polym. 69 (2007) 142–147. https://doi.org/10.1016/j.carbpol.2006.09.010.
[20] D.H.K. Reddy, S.M. Lee, Adv. Colloid Interface Sci. 68 (2013) 201–202. http://doi.org/10.1016/j.cis.2013.10.002.
[21] G.R. Mahdavinia, M. Soleymani, M. Nikkhoo, S.M.F. Farnia, M. Aminia, New J. Chem. 41 (2017) 3821–3828. http://doi.org/10.1039/c6nj03862j.
[22] G.M. Raghavendra, J. Jung, D. Kim, J. Seo, Carbohydr. Polym. 172 (2017) 78–84. http://doi.org/10.1016/j.carbpol.2017.04.070.
[23] J.F. de Souza, G.T. da Silva, A.R. Fajardo, Carbohydr. Polym. 161 (2017) 187–196. http://doi.org/10.1016/j.carbpol.2017.01.018.
[24] A. Murugadoss, A. Chattopadhyay, Nanotechnology 19 (2008) 1–9. http://doi.org/10.1088/0957-4484/19/01/015603.
[25] K. Karakas, A. Celebioglu, M. Celebi, T. Uyar, M. Zahmakiran, Appl. Catal. B Environ. 203 (2017) 549–562. http://doi.org/10.1016/j.apcatb.2016.10.020.
[26] J. Safari, Z. Zarnegar, Int. J. Biol. Macromol. 75 (2015) 21–31. http://doi.org/10.1016/j.ijbiomac.2015.01.013.
[27] A. Naghipour, A. Fakhri, Catal. Commun. 73 (2016) 39–45. https://doi.org/10.1016/j.catcom.2015.10.002.
[28] M. Misono, L. Ono, G. Koyano, A. Aoshima, Pure Appl. Chem. 72 (2000) 1305–1311. http://doi.org/10.1016/j.carres.2012.02.021.
[29] M.M. Heravi, G. Rajabzadeh, F.F. Bamoharram, N. Seifi, J. Mol. Catal. Chem. 256 (2006) 238–241. https://doi.org/10.1016/j.molcata.2006.04.016.
[30] M.M. Heravi, G. Rajabzadeh, F.F. Bamoharram, N. Seifi, J. Mol. Catal. Chem. 259 (2006) 213–217. https://doi.org/10.1016/j.molcata.2006.06.037.
[31] M.T. Pope, Heteropoly and Isopoly Oxometalates, Springer Verlag, New York, 1983, pp. 23–27.
[32] M.M. Heravi, G. Rajabzadeh, F.F. Bamoharram, Catal. Commun. 7 (2006)

499–501. https://doi.org/10.1016/j.catcom.2006.01.003.
[33] S.S. Wang, G.Y. Yang, Chem. Rev. 115 (2015) 4893–4962. https://doi.org/10.1021/cr500390v.
[34] M.T. Pope, Heteropoly and Isopoly Oxometalates, Springer-Verlag, Berlin, 1983, 730–730.
[35] J. Safari, S.H. Banitaba, S. Dehghan Khalili, Ultrason. Sonochem. 19 (2012) 1061–1069. https://doi.org/10.1016/j.ultsonch.2012.01.005.
[36] N.G. Khaligh, F. Shirini, Ultrason. Sonochem. 20 (2013) 19–25. https://doi.org/10.1016/j.ultsonch.2012.07.016.
[37] S.R. Kanth, G.V. Reddy, K.H. Kishore, P.S. Rao, B. Narsaiah, U.S.N. Murthy, Eur. J. Med. Chem. 41 (2006) 1011–1016. https://doi.org/10.1016/j.ejmech.2006.03.028.
[38] L.R. Bennett, C.J. Blankley, R.W. Fleming, R.D. Smith, D.K. Tessman, J. Med. Chem. 24 (1981) 382–389. https://doi.org/10.1021/jm00136a006.
[39] P.N. Sudhan, M. Ghashang, S.S. Mansoor, Beni-Suef Univ. J. Basic Appl. Sci. 5 (2016) 340–349. http://doi.org/10.1016/j.bjbas.2016.11.004.
[40] G.K. Verma, K. Raghuvanshi, R. Kumar, M.S. Singh, Tetrahedron Lett. 53 (2012) 399–402. http://doi.org/10.1016/j.bjbas.2016.11.004.
[41] J.M. Khurana, A. Chaudhary, B. Nand, A. Lumb, Tetrahedron Lett. 53 (2012) 3018–3022. https://doi.org/10.1016/j.tetlet.2012.04.001.
[42] S. Abdolmohammadi, S. Balalaie, M. Barari, F. Rominger, Comb. Chem. High Throughput Screen. 16 (2013) 150–159. https://doi.org/10.2174/1386207113804806319.
[43] F. Nemati, R. Saeedirad, Chin. Chem. Lett. 24 (2013) 370–372. https://doi.org/10.1016/j.cclet.2013.02.018.
[44] C.C. Lin, Y. Guo, J. Vela, ACS Catal. 5 (2015) 1037–1044. https://doi.org/10.1021/cs501650j.
[45] R.C. Deltcheff, M. Fournier, R. Franck, R. Thouvenot, Inorg. Chem. 22 (1983) 207–216. https://doi.org/10.1021/ic00144a006.
[46] M. Yamada, A. Maeda, Polymer 50 (2009) 6076–6082. https://doi.org/10.1016/j.polymer.2009.10.043.
[47] S.M. Sadeghzadeh, RSC Adv. 6 (2016) 75973–75980. https://doi.org/10.1039/c6ra15766a.